

## A Novel Anionic Inward Rectifier in Native Cardiac Myocytes

Dayue Duan, Lingyu Ye, Fiona Britton, Burton Horowitz, Joseph R. Hume

**Abstract**—Although the cationic inward rectifiers (Kir and hyperpolarization-activated  $I_f$  channels) have been well characterized in cardiac myocytes, the expression and physiological role of anionic inward rectifiers in heart are unknown. In the present study, we report the functional and molecular identification of a novel chloride ( $\text{Cl}^-$ ) inward rectifier ( $I_{\text{Cl.ir}}$ ) in mammalian heart. Under conditions in which cationic inward rectifier channels were blocked, membrane hyperpolarization ( $-40$  to  $-140$  mV) activated an inwardly rectifying whole-cell current in mouse atrial and ventricular myocytes. Under isotonic conditions, the current activated slowly with a biexponential time course (time constants averaging  $179.7 \pm 23.4$  [mean  $\pm$  SEM] and  $2073.6 \pm 287.6$  ms at  $-120$  mV). Hypotonic cell swelling accelerated the activation and increased the current amplitude whereas hypertonic cell shrinkage inhibited the current. The inwardly rectifying current was carried by  $\text{Cl}^-$  ( $I_{\text{Cl.ir}}$ ) and had an anion permeability sequence of  $\text{Cl}^- > I^- \gg$  aspartate.  $I_{\text{Cl.ir}}$  was blocked by 9-anthracene-carboxylic acid and cadmium but not by stilbene disulfonates and tamoxifen. A similar  $I_{\text{Cl.ir}}$  was also observed in guinea pig cardiac myocytes. The properties of  $I_{\text{Cl.ir}}$  are consistent with currents generated by expression of CIC-2  $\text{Cl}^-$  channels. Reverse transcription polymerase chain reaction and Northern blot analysis confirmed transcriptional expression of CIC-2 in both atrial and ventricular tissues and isolated myocytes of mouse and guinea pig hearts. These results indicate that a novel  $I_{\text{Cl.ir}}$  is present in mammalian heart and support a potentially important role of CIC-2 channels in the regulation of cardiac electrical activity and cell volume under physiological and pathological conditions. The full text of this article is available at <http://www.circresaha.org>. (*Circ Res.* 2000;86:e63-e71.)

**Key Words:** channel,  $\text{Cl}^-$  ■ action potential ■ cell volume

At least six distinct types of sarcolemmal  $\text{Cl}^-$  currents have been functionally identified in cardiac myocytes.<sup>1-5</sup> These include  $\text{Cl}^-$  currents activated by intracellular cAMP-PKA ( $I_{\text{Cl.PKA}}$ ), PKC ( $I_{\text{Cl.PKC}}$ ), intracellular  $\text{Ca}^{2+}$  ( $I_{\text{Cl.Ca}}$  or  $I_{\text{to2}}$ ), extracellular ATP ( $I_{\text{Cl.ATP}}$ ), cell volume ( $I_{\text{Cl.vol}}$ ), and a basally active  $\text{Cl}^-$  current ( $I_{\text{Cl.b}}$ ). It has been well established that  $I_{\text{Cl.PKA}}$  is mediated by cardiac expression of an isoform of the epithelial cystic fibrosis transmembrane conductance regulator (CFTR)  $\text{Cl}^-$  channel,<sup>6-8</sup> and recent data suggest that  $I_{\text{Cl.vol}}$  and  $I_{\text{Cl.b}}$  may be attributed to cardiac expression of a member of the CIC  $\text{Cl}^-$  channel superfamily,<sup>9</sup> CIC-3.<sup>10,11</sup> Functional data suggest that  $I_{\text{Cl.PKC}}$  and  $I_{\text{Cl.ATP}}$  may also be attributed to activation of CFTR  $\text{Cl}^-$  channels.<sup>12-16</sup> Although the molecular entity responsible for  $I_{\text{Cl.Ca}}$  remains to be determined, it may be encoded by a member of the new CLCA gene family.<sup>17</sup> With physiological  $\text{Cl}^-$  gradients, all of these  $\text{Cl}^-$  currents activate predominantly at depolarized voltages, exhibit outward rectification, and thus contribute significantly to shortening of action potential duration; although activation of  $I_{\text{Cl.Ca}}$  under conditions of intracellular  $\text{Ca}^{2+}$  overload may, in addition, contribute to the development of oscillatory delayed afterdepolarizations.<sup>3,5</sup>

Recently, another member of the CIC  $\text{Cl}^-$  channel family, CIC-2, has been cloned originally from rat heart and brain<sup>18</sup> and then from rabbit heart.<sup>19</sup> Although it has been shown that functional expression of rat CIC-2 (rCIC-2) and rabbit cardiac CIC-2 (CIC-2 $\alpha$ ) mRNA in *Xenopus* oocytes gives rise to an inwardly rectifying, hyperpolarization-activated  $\text{Cl}^-$  conductance that is modulated by changes in cell volume and extracellular pH,<sup>18-20</sup> inwardly rectifying hyperpolarization-activated  $\text{Cl}^-$  currents with properties resembling CIC-2 have yet to be identified in native cardiac myocytes. However, hyperpolarization-activated CIC-2 channels expressed in heterologous expression systems bear a striking resemblance to the well-characterized hyperpolarization-activated cationic pacemaker current,  $I_f$  (or  $I_h$ ), found in many mammalian cardiac cell types<sup>21,22</sup> and are now known to belong to the HCN gene family.<sup>23-25</sup> Because of similarities in inward rectification and relatively slow activation during membrane hyperpolarization, it is possible that coexpression of CIC-2  $\text{Cl}^-$  channels in some native cardiac myocytes, which also express  $I_f$  (HCN), may in part explain earlier observations that suggested some anion sensitivity of the hyperpolarization-activated  $I_f$ .<sup>26-28</sup>

Received January 17, 2000; accepted February 1, 2000.

From the Department of Physiology and Cell Biology, University of Nevada School of Medicine, Reno, Nev.

Correspondence to Dayue Duan, MD, PhD, Department of Physiology and Cell Biology/351, University of Nevada School of Medicine, Reno, NV 89557-0046. E-mail [dduan@med.unr.edu](mailto:dduan@med.unr.edu)

© 2000 American Heart Association, Inc.

*Circulation Research* is available at <http://www.circresaha.org>

In the present study, using both electrophysiological and molecular biological techniques, we tested the hypothesis that endogenous expression of CIC-2 may be responsible for a novel, inwardly rectifying hyperpolarization-activated anion conductance in native atrial and ventricular myocytes isolated from mouse and guinea pig hearts. The data demonstrate that, under conditions during which cationic inwardly rectifying channels are blocked or eliminated, inwardly rectifying currents with an anion permeability of  $\text{Cl}^- > I^- \gg \text{aspartate} (\text{Asp}^-)$  can be detected in a percentage of mouse and guinea pig atrial and ventricular myocytes. The biophysical and pharmacological properties of this inwardly rectifying  $\text{Cl}^-$  current ( $I_{\text{Cl,ir}}$ ) are nearly identical to the known properties of cloned CIC-2  $\text{Cl}^-$  channels expressed in heterologous expression systems. Finally, we present evidence using the reverse transcription–polymerase chain reaction (RT-PCR) and Northern blot analysis that confirms transcriptional expression of a CIC-2 homologue in both atrial and ventricular tissue and cells from mouse and guinea pig heart. These results provide the first evidence that a novel  $I_{\text{Cl,ir}}$ , which may be encoded by CIC-2, is functionally expressed in mammalian heart.  $I_{\text{Cl,ir}}$ , like cationic inward rectifiers, may play an important role in the regulation of action potential duration, resting membrane potential, and pacemaker activity under both physiological and pathophysiological conditions. A preliminary report describing these results has been published.<sup>29</sup>

## Materials and Methods

### Electrophysiological Measurements

Whole-cell currents were measured from single atrial and ventricular myocytes enzymatically isolated from mouse and guinea pig hearts using the tight-seal, whole-cell, voltage-clamp technique,<sup>30</sup> as previously described.<sup>16,31</sup> To prevent contamination from  $\text{Ca}^{2+}$  and  $\text{K}^+$  currents, and the cationic inward rectifiers  $I_{\text{K1}}$  and  $I_{\text{f}}$ , nisoldipine (1  $\mu\text{mol/L}$ ), 4-aminopyridine (4-AP, 2 mmol/L),  $\text{Ba}^{2+}$  (2 mmol/L), and  $\text{Cs}^+$  (10 mmol/L) were present continuously in the extracellular bath solutions and cations in the intracellular pipette solution and, in some experiments, in the bath solution were replaced by the large impermeant cation, *N*-methyl-D-glucamine (NMDG). Hypotonic (230 mOsm/kg  $\text{H}_2\text{O}$ , measured by freezing-point depression) bath solutions contained (mmol/L) NaCl 100,  $\text{MgCl}_2$  1,  $\text{CaCl}_2$  1,  $\text{BaCl}_2$  2,  $\text{NaH}_2\text{PO}_4$  0.33, CsCl 10, HEPES 10, glucose 5.5,  $[\text{Cl}^-]_i$  118; pH 7.4. In some experiments, NaCl was replaced with equimolar concentrations (100 mmol/L) of NaI or Na-aspartate. The isotonic and hypertonic bath solutions were the same as the hypotonic solution except the osmolarity was adjusted to 290 mOsm/kg  $\text{H}_2\text{O}$  and 360 mOsm/kg  $\text{H}_2\text{O}$  by adding mannitol. The pipette solution contained (in mmol/L) NMDG-Cl 118,  $\text{MgATP}$  5,  $\text{NaGTP}$  0.1, ethylene-glycobis( $\beta$ -aminoethyl ether)-*N,N,N',N'*-tetraacetic acid (EGTA) 5, HEPES 5,  $[\text{Cl}^-]_i$  118; pH 7.4, 290 mOsm/kg  $\text{H}_2\text{O}$  using mannitol. In low  $[\text{Cl}^-]_i$  (20 mmol/L) pipette solution, 98 mmol/L NMDG-Cl was replaced by NMDG-aspartate. A bridge (3 mol/L KCl in agar salt) between the bath and a Ag/AgCl reference electrode immersed in pipette solution was used to minimize changes in liquid junction potential, and junction potentials were zeroed before formation of the membrane-pipette seal. Cell dimensions (length and width) were roughly estimated with a calibrated graticule in the microscope eyepiece. Experiments were conducted at room temperature (22°C to 24°C).

### Reverse Transcription–Polymerase Chain Reaction (RT-PCR)

RT-PCR of total RNA prepared from cardiac tissues using the Trizol reagent (Life Technologies) or from enzymatically dispersed indi-

vidual cardiac myocytes using SNAP total RNA isolation kit (Invitrogen) was performed as previously described.<sup>10</sup> The primer region (forward: 5'-TGGGAGGAGCAGCAGCTGAA-3', reverse: 5'-CAGAGTGCATGCACCTCT-GTGGT-3') is specific for rCIC-2 (GenBank accession No. X64139)<sup>20</sup> and corresponds to nucleotides 2515 to 2822, generating a 307-nucleotide amplification product. Automatic nucleotide sequencing was performed on both strands using the dideoxy nucleotide chain termination method (Genetic Analyzer, Model 310, Perkin Elmer).

### Northern Blot Analysis

To confirm the expression of CIC-2 in cardiac tissues, Northern blot analysis was performed as described previously.<sup>10,16</sup> A 420-bp rCIC-2 cDNA probe was radiolabeled with <sup>32</sup>P by random priming.<sup>32</sup> Hybridization was performed under the same conditions overnight. The filters were washed at high stringency (3 times in  $2\times$  SSC at room temperature for 5 minutes then twice in  $0.2\times$  SSC/0.1% SDS at 65°C for 30 minutes) to ensure specificity of labeling. Filters were exposed to film, and autoradiography was performed using a BioRad phosphorimager (Hercules).

### Data Analysis

Data are presented as mean  $\pm$  SEM. Student's *t* test or ANOVA with Scheffé contrasts was used to determine statistical significance. A two-tailed probability (*P*) of  $\leq 5\%$  was considered significant.

## Results

### Novel Volume-Regulated Inward Rectifier $\text{Cl}^-$ Current ( $I_{\text{Cl,ir}}$ ) in Mouse Heart

With the cationic inward rectifier blockers ( $\text{Cs}^+$  10 mmol/L and  $\text{Ba}^{2+}$  2 mmol/L) in the extracellular bath solution and a large impermeable cation NMDG in the intracellular pipette solution to replace all permeable cations, hyperpolarization of the cell membrane activated a time-dependent inward current in both atrial and ventricular myocytes isolated from mouse heart. Figure 1A shows an example of the currents recorded from ventricular myocytes under isotonic, hypotonic, and hypertonic conditions. The current activated on hyperpolarization from  $-40$  to  $-140$  mV under isotonic (290 mOsm/kg  $\text{H}_2\text{O}$ ) conditions. Subsequent exposure of the same cells to hypotonic (230 mOsm/kg  $\text{H}_2\text{O}$ , 21% hypotonic) bath solutions caused significant cell swelling and caused a further increase in current amplitude (Figure 1). Overall, cell areas during hypotonic cell swelling were estimated to increase from  $1633 \pm 165$  to  $2234 \pm 176 \mu\text{m}^2$  ( $n=5$ ,  $P<0.05$ ). Hypotonic cell swelling not only increased current amplitudes but also accelerated the kinetics of current activation. As shown in Figure 1B, the time-dependent activation of the current at hyperpolarized potentials was relatively slow in onset and could be best fit by a biexponential function. Under isotonic conditions (left panel of Figure 1B), the mean activation time constants at  $-120$  mV were  $\tau_1=179.7 \pm 23.4$  ms and  $\tau_2=2073.6 \pm 287.6$  ms ( $n=5$ ). Under hypotonic conditions (right panel of Figure 1B), both the fast activation time constant ( $\tau_1=97.5 \pm 8.5$  ms at  $-120$  mV,  $n=5$ ,  $P=0.011$  versus isotonic condition) and the slow activation time constant ( $\tau_2=656.4 \pm 113.6$  ms at  $-120$  mV,  $P=0.002$  versus isotonic condition) were significantly reduced. Hypertonic cell shrinkage caused inhibition of the current (Figures 1A and 1C). Under isotonic conditions, we observed similar hyperpolarization-activated currents in 5 of 52 (9.6%) ventricular myocytes, which was further regulated by hypotonic

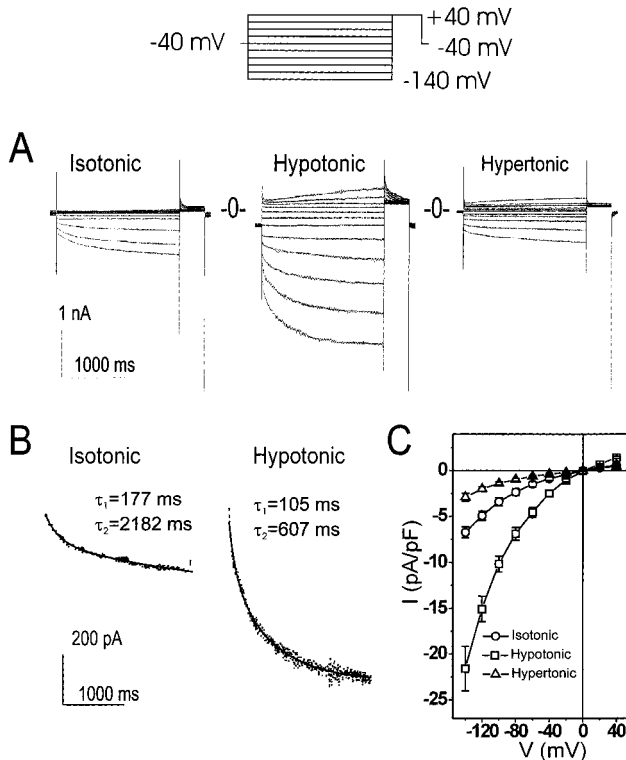


**Figure 1.** Hyperpolarization-activated anion current and its sensitivity to cell volume in mouse ventricular myocytes. Currents were recorded using voltage-clamp protocols shown on top. Cells were held at  $-40$  mV, and test potentials were applied from  $-140$  to  $+40$  mV in  $+20$ -mV increments for 2 seconds and then to  $+40$  mV for 400 ms before return to the holding potential. The test potentials were applied at an interval of 10 seconds (insert on the top). A, Hyperpolarization voltage pulses activated inward currents under isotonic conditions (left panel). Subsequent exposure of the same cell to hypotonic solution (0.79T) caused a further increase in current amplitudes (middle panel). Further exposure of the cell to hypertonic solution caused a decrease in current amplitudes (right panel). B, Effects of hypotonic cell swelling on the time course of activation of the inward rectifying current. Representative current recordings from one cell after hyperpolarization to  $-120$  mV under isotonic (left panel) and hypotonic (right panel) conditions, respectively, are shown. The points represent current activation data, and the solid lines are least-square curve fits obtained with the curve-fitting program Clampfit (Axon Instruments). The activation process was best fit to a biexponential function with a fast time constant ( $\tau_1$ ) of 177 ms and a slow time constant ( $\tau_2$ ) of 2182 ms under isotonic conditions. Hypotonic cell swelling increased the amplitude of the current and also accelerated the activation kinetics ( $\tau_1=105$  ms,  $\tau_2=607$  ms). C, Mean  $I$ - $V$  relationship from 5 different cells under isotonic ( $\circ$ ), hypotonic ( $\square$ ), and hypertonic ( $\triangle$ ) conditions. Currents were measured at the end of each 2-second test pulse. Mean reversal potentials ( $E_{rev}$ ) of the currents under isotonic, hypotonic, and hypertonic conditions were  $2.0 \pm 3.8$  mV,  $3.3 \pm 3.4$  mV, and  $-1.7 \pm 3.3$  mV ( $n=5$ ,  $P=NS$ ), respectively, which were very close to the predicted equilibrium potential of  $Cl^-$  ( $E_{Cl}=0$  mV) with a symmetrical  $Cl^-$  gradient ( $[Cl^-]_o/[Cl^-]_i=118/118$  mmol/L).

cell swelling and hypertonic cell shrinkage. Figure 1C shows the mean current-voltage ( $I$ - $V$ ) relationship of the hyperpolarization-activated inward currents under isotonic ( $\circ$ ), hypotonic ( $\square$ ), and hypertonic ( $\triangle$ ) conditions. These currents had a strong inwardly rectifying  $I$ - $V$  relationship with mean reversal potentials ( $E_{rev}$ ) of  $2.0 \pm 3.8$  mV,  $3.3 \pm 3.4$  mV, and  $-1.7 \pm 3.3$  mV ( $n=5$ ,  $P=NS$ ), under isotonic, hypotonic, and

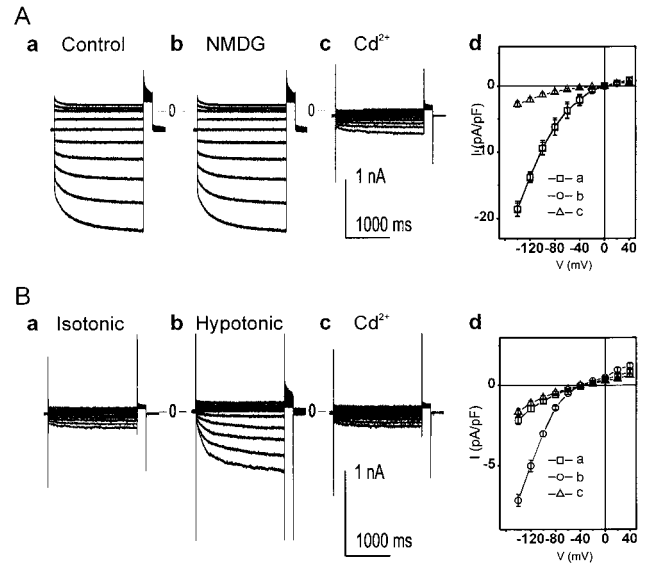


**Figure 2.** Ion selectivity of hyperpolarization-activated currents in mouse ventricular myocytes. Currents were recorded using voltage-clamp protocols shown on top of Figure 1. A-a, Current tracings recorded from a mouse ventricular myocyte in standard hypotonic bath solution (Control), which contained  $Na^+$ ,  $Ba^{2+}$ ,  $Ca^{2+}$ , and  $Cs^+$  (see Materials and Methods). A-b, Current tracings recorded from the same cell after exposure to hypotonic solution in which all cations were replaced with an impermeable large cation NMDG. A-c, Further exposure of the cell to hypotonic NMDG solution that contained 0.3 mmol/L cadmium ( $Cd^{2+}$ ) caused a decrease in current amplitudes. A-d, Mean  $I$ - $V$  relationship from 3 different cells under hypotonic control ( $\square$ ), hypotonic NMDG ( $\circ$ ), and hypotonic NMDG+ $Cd^{2+}$  ( $\triangle$ ) conditions. Substitution of cations in extracellular bath solution failed to alter the  $I$ - $V$  relationship and reversal potential ( $-1.2 \pm 3.4$  mV vs  $0.4 \pm 2.4$  mV,  $n=3$ ,  $P=NS$ ) of the inwardly rectifying currents. B-a, Current tracings recorded from a mouse ventricular myocyte in standard isotonic bath solution (Isotonic) with  $Cl^-$  in intracellular pipette solution partially replaced by  $Asp^-$  (total  $[Cl^-]_i=20$  mmol/L). B-b, Current tracings recorded from the same cell after exposure to standard hypotonic solution (Hypotonic). B-c, Further exposure of the cell to hypotonic solution that contained 0.3 mmol/L ( $Cd^{2+}$ ) caused a decrease in current amplitudes. B-d, Mean  $I$ - $V$  relationship from 4 different cells under isotonic ( $\square$ ), hypotonic ( $\circ$ ), and hypotonic  $Cd^{2+}$  ( $\triangle$ ) conditions. Compared with the currents recorded with high (118 mmol/L)  $[Cl^-]_i$  (see panel A and Figure 1), reduction in  $[Cl^-]_i$  reduced the current density of the hypotonic cell swelling-activated inward current and shifted the reversal potential of the current to a more negative potential ( $-43.8 \pm 1.6$  mV,  $n=4$ ), which is very close to the predicted  $E_{Cl}$  ( $-45.6$  mV).

hypertonic conditions, respectively, which were very close to the predicted equilibrium potential of  $Cl^-$  ( $E_{Cl}=0$  mV) with a symmetrical  $Cl^-$  gradient ( $[Cl^-]_o/[Cl^-]_i=118/118$  mmol/L).

As shown in Figure 2A, the time-dependent inwardly rectifying currents in mouse ventricular myocytes remained unchanged when all cations in the extracellular solution were also replaced by NMDG. These currents, however, were significantly reduced by extracellular cadmium (0.3 mmol/L), which has been shown to block inwardly rectifying  $Cl^-$  current in noncardiac cells.<sup>33,34</sup> Furthermore, as shown in Figure 2B, when  $[Cl^-]_i$  was partially substituted with equimolar  $Asp^-$  (98 mmol/L;  $[Cl^-]_i$  20 mmol/L), the hypotonic cell swelling-activated inward current was significantly smaller than the current recorded with high  $[Cl^-]_i$  (see Figures 1 and 2A), and the reversal potential of the current shifted to more

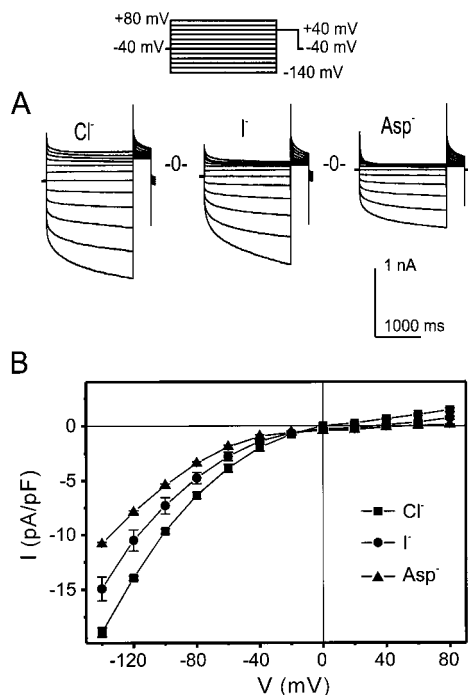


**Figure 3.** Anion selectivity of hypotonic cell swelling-activated  $I_{Cl,ir}$  in mouse atrial myocytes. A, Representative whole-cell currents recorded in high extracellular  $Cl^-$  ( $[Cl^-]_o = 118$  mmol/L) bath solution (left),  $[Cl^-]_o$  were reduced to 18 mmol/L ( $E_{Cl} 48.3$  mV) by equimolar (100 mmol/L) replacement of  $Cl^-$  with  $I^-$  (middle) or  $Asp^-$  (right). Currents were recorded using voltage-clamp protocols shown on top. Cells were held at  $-40$  mV, and test potentials were applied from  $-140$  to  $+80$  mV in  $+20$ -mV increments for 2 seconds and then to  $+40$  mV for 400 ms before return to the holding potential. The test potentials were applied at an interval of 10 seconds. B, Mean  $I$ - $V$  relationships of swelling-activated  $I_{Cl,ir}$  before (■) and after  $[Cl^-]_o$  was substituted by  $I^-$  (●) or  $Asp^-$  (▲).  $I^-$  and  $Asp^-$  substitution of  $Cl^-$  shifted the reversal potential of  $I_{Cl,ir}$  from  $+3.5 \pm 0.7$  mV ( $Cl^-$ ) to  $+33.4 \pm 4.6$  mV ( $I^-$ ) and  $+47.2 \pm 1.2$  mV ( $Asp^-$ ) ( $n=4$ ), respectively.

negative potential with a mean value of  $-43.8 \pm 1.6$  mV ( $n=4$ ), which is very close to the predicted  $E_{Cl}$  ( $-45.5$  mV). Again, these currents were significantly blocked by extracellular cadmium. These results strongly indicate that the current in mouse ventricular myocytes is neither  $I_f$  nor a swelling-induced nonspecific cationic inward rectifier current.<sup>35,36</sup> It may represent a novel volume-regulated  $Cl^-$  inward rectifier current,  $I_{Cl,ir}$ .

Similar  $I_{Cl,ir}$  was also observed in mouse atrial myocytes (16 of 113, 14.2%). The relative anion selectivity of  $I_{Cl,ir}$  was further examined by replacing  $[Cl^-]_o$  with an equimolar concentration (100 mmol/L) of iodide ( $I^-$ ) or aspartate ( $Asp^-$ ) ( $E_{Cl} 48.3$  mV) under hypotonic conditions. Cells were held at  $-40$  mV, and test potentials were applied at an interval of 10 seconds from  $-140$  mV to  $+80$  mV for 2 seconds in  $+20$ -mV increments and then to  $+40$  mV for 400 ms before return to the holding potential (see Figure 3 and inset). In four different mouse atrial cells, reduction of  $[Cl^-]_o$  caused a shift of  $E_{rev}$  of the current from  $+3.5 \pm 0.7$  mV ( $Cl^-$ ) to  $+33.4 \pm 4.6$  mV ( $I^-$ ) and  $+47.2 \pm 1.2$  mV ( $Asp^-$ ), respectively. The permeability ratios (permeability ratio of anion X with respect to  $Cl^-$ ,  $P_X/P_{Cl}$ ) were then calculated from the shifts of  $E_{rev}$  using the modified Goldman-Hodgkin-Katz equation.<sup>37</sup>

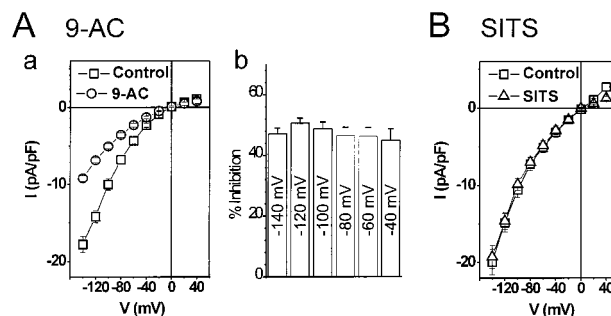


**Figure 4.** Effects of  $Cl^-$  channel blockers on  $I_{Cl,ir}$ . Currents were recorded using the same protocol as shown in Figure 1. A, Carboxylic acid derivative 9-AC blocked  $I_{Cl,ir}$  in mouse atrial myocytes. A-a, Mean  $I$ - $V$  curves of  $I_{Cl,ir}$  obtained from 4 different mouse atrial cells under hypotonic control condition (□) and after 1 mmol/L 9-AC (○). A-b, Percentage of current inhibition by 9-AC at various test potentials. The inhibition of the current by 9-AC showed no voltage dependence. B, Mean  $I$ - $V$  curves of  $I_{Cl,ir}$  obtained from 5 different mouse atrial cells under hypotonic control condition (□) and after exposed to 1 mmol/L SITS (△). The disulfonic stilbene derivative SITS failed to affect  $I_{Cl,ir}$  in mouse atrial myocytes.

The cell swelling-activated inward rectifier channel had an estimated  $P_I/P_{Cl}$  of  $0.22 \pm 0.09$  ( $n=4$ ) and  $P_{Asp}/P_{Cl}$  of  $0.04 \pm 0.01$  ( $n=4$ ), suggesting that the current is conducted through an anion selective channel with a relative anion permeability of  $Cl^- > I^- \gg Asp^-$ .

#### Effects of $Cl^-$ Channel Blockers on $I_{Cl,ir}$

Several compounds including arylaminoalkyl benzoates derivatives such as 9-anthracene-carboxylic acid (9-AC) and disulfonic stilbene derivatives such as 4-acetamido-4'-isothiocyanatostilbene-2,2'-disulfonic acid (SITS) have been identified as effective blockers of a variety of cardiac<sup>5,38,39</sup> and noncardiac  $Cl^-$  channels.<sup>40</sup> Therefore, we assessed the effects of 9-AC and SITS on the swelling-induced  $I_{Cl,ir}$  in mouse atrial myocytes. As shown in Figure 4A, 1 mmol/L of 9-AC significantly ( $P < 0.001$  versus control at all test potentials) blocked  $I_{Cl,ir}$  (Figure 4A-a) in a voltage-independent manner (Figure 4A-b). The inhibition of the current amplitude at test potentials of  $-140$ ,  $-120$ ,  $-100$ ,  $-80$ ,  $-60$ , and  $-40$  mV was  $47.1 \pm 1.9\%$ ,  $50.6 \pm 1.7\%$ ,  $48.8 \pm 2.2\%$ ,  $46.6 \pm 2.7\%$ ,  $46.3 \pm 2.9\%$ , and  $45.0 \pm 3.8\%$ , respectively ( $n=4$ ,  $P=NS$  for voltage dependence). In contrast,  $I_{Cl,ir}$  was not sensitive to disulfonic stilbene derivatives. As shown in Figure 4B, 1 mmol/L SITS failed to affect the current in mouse atrial cells. The changes in current densities after SITS were  $-3.0 \pm 1.7\%$ ,  $-1.3 \pm 2.6\%$ ,  $-6.2 \pm 4.4\%$ ,  $-2.3 \pm 3.5\%$ ,  $-4.2 \pm 1.6\%$ , and  $-5.4 \pm 4.0\%$  at test potentials of  $-140$ ,  $-120$ ,  $-100$ ,  $-80$ ,  $-60$ , and  $-40$  mV, respectively ( $n=5$ ,  $P=NS$  versus control at all test potentials).

#### $I_{Cl,ir}$ in Guinea Pig Cardiac Myocytes

Hyperpolarization-activated inwardly rectifying, volume-sensitive, stilbene-insensitive currents with properties similar to mouse cardiac  $I_{Cl,ir}$  were also observed in some guinea pig atrial (6 of 56, 10.7%) and ventricular (3 of 32, 9.4%) myocytes. Under hypotonic conditions, it has been reported that an outwardly rectifying volume-regulated  $Cl^-$  current ( $I_{Cl,vo}$ ) is present in  $\approx 90\%$  of atrial myocytes and  $\approx 30\%$  of



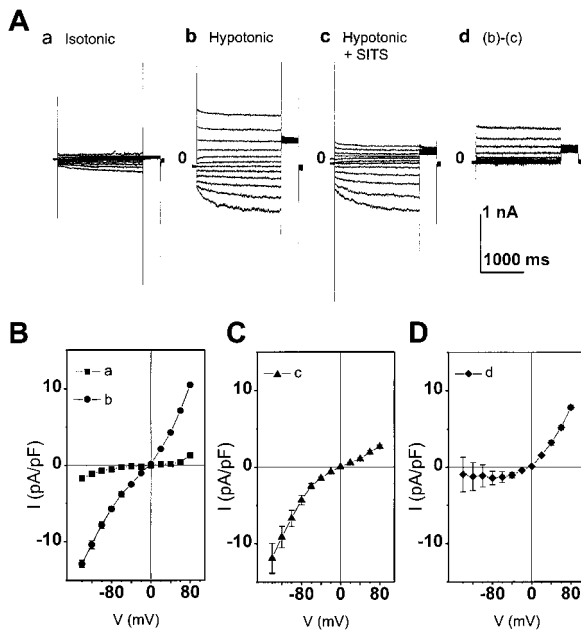


**Figure 5.** Volume-regulated whole-cell anion currents in guinea pig ventricular myocytes. Currents were recorded using the same protocols as shown in Figure 3. A, Representative whole-cell currents recorded under isotonic (A-a), hypotonic (A-b), and hypotonic 1 mmol/L SITS (A-c) conditions. Panel A-d shows the SITS-sensitive difference current obtained by subtracting the current in panel A-c from the current in panel A-b. SITS inhibited mainly the volume-regulated, outwardly rectifying  $\text{Cl}^-$  current ( $I_{\text{Cl.vol}}$ ; see text). B, Mean  $I$ - $V$  curves of whole-cell currents obtained from 3 different guinea pig ventricular myocytes under isotonic (■) and hypotonic (●) conditions. C, Mean  $I$ - $V$  curve of SITS-insensitive whole-cell currents, which exhibited strong inward rectification. D, Mean  $I$ - $V$  curve of SITS-sensitive currents, which exhibited strong outward rectification.

ventricular myocytes of guinea pig heart.<sup>31,41–44</sup> Different from  $I_{\text{Cl.ir}}$ , however,  $I_{\text{Cl.vol}}$  is outwardly rectifying, deactivates at positive potentials, has an anion permeability sequence of  $I^- > \text{Cl}^-$ , and is sensitive to disulfonic stilbene (such as SITS)  $\text{Cl}^-$  channel blockers.<sup>31,41,42,44</sup> Figure 5A shows an example of whole-cell currents recorded from a guinea pig ventricular myocyte, in which both  $I_{\text{Cl.vol}}$  and  $I_{\text{Cl.ir}}$  were activated under hypotonic conditions. In these experiments, currents were recorded using the same bath and pipette solutions as in Figure 1 and the same voltage-clamp protocol as in Figure 3. As shown in Figure 5A-a, small hyperpolarization-activated time-dependent inward currents could be detected in this cell even under isotonic conditions. Subsequent hypotonic cell swelling not only increased the inward currents but also activated large outward currents (Figure 5A-b). Although the outward currents showed time-dependent deactivation at positive depolarizing potentials, the inward currents showed time-dependent activation at negative membrane potentials. Subsequent exposure of the same cell to 1 mmol/L of SITS, an effective blocker of cardiac  $I_{\text{Cl.vol}}$ , caused an inhibition of mainly the outward current (Figure 5A-d), leaving the time-dependent inward current largely unaffected (Figure 5A-c). Similar results were observed in three guinea pig ventricular myocytes, and the mean  $I$ - $V$  curves under isotonic (■), hypotonic (●), and hypotonic 1 mmol/L SITS (▲) conditions are shown in Figures 5B and 5C, respectively. The SITS-

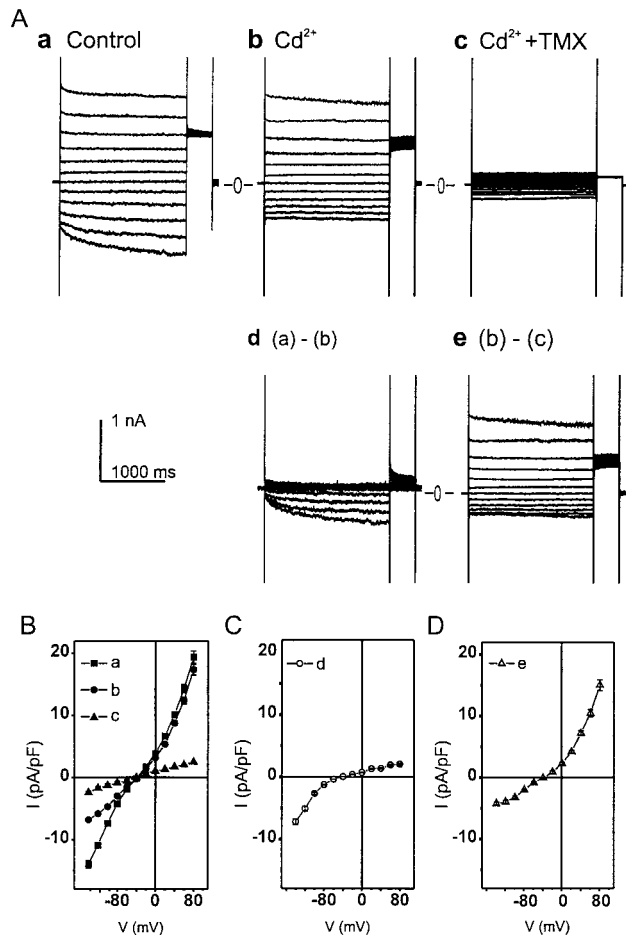
sensitive current showed outward rectification and deactivation at more positive potentials (Figures 5A-d and 5D), which are typical features of  $I_{\text{Cl.vol}}$ .<sup>10,31,42</sup> The SITS-insensitive inwardly rectifying current (Figures 5A-c and 5C), however, had properties very similar to those of  $I_{\text{Cl.ir}}$  observed in mouse cardiac myocytes described earlier in Figure 1. The estimated current densities for guinea pig  $I_{\text{Cl.ir}}$  in ventricular myocytes ( $-10.4 \pm 0.5$  pA/pF, at  $-120$  mV,  $n=3$ ) and atrial myocytes ( $-12.8 \pm 0.7$  pA/pF, at  $-120$  mV,  $n=3$ ) revealed no significant differences ( $P=NS$ ).

We also examined the  $\text{Cl}^-$  dependence of the current in guinea pig atrial myocytes using different  $[\text{Cl}^-]_i$ . As shown in Figure 6A-a, when  $[\text{Cl}^-]_i$  was reduced to 20 mmol/L by replacing NMDG-Cl with equimolar amount (98 mmol/L) of NMDG-aspartate, hypotonic cell swelling induced an activation of both small slowly activating inward currents and large outward currents (Figure 6A-a). Subsequent exposure of the same cell to the  $I_{\text{Cl.ir}}$  blocker  $\text{Cd}^{2+}$  (0.3 mmol/L) caused an inhibition of mainly the inward currents (Figures 6A-b and 6A-d). Further exposure of the cell to 10  $\mu\text{mol/L}$  of tamoxifen (TMX), which blocks  $I_{\text{Cl.vol}}$  in many cardiac and noncardiac cells<sup>10,11,33,41</sup> but has no effect on  $I_{\text{Cl.ir}}$  in noncardiac cells,<sup>33</sup> caused a further inhibition of the currents (Figures 6A-c). Similar results were observed in three guinea pig atrial myocytes, and the mean  $I$ - $V$  curves under hypotonic control (■), hypotonic+0.3 mmol/L  $\text{Cd}^{2+}$  (●), and hypotonic+0.3 mmol/L  $\text{Cd}^{2+}$ +10  $\mu\text{mol/L}$  TMX (▲) conditions, respectively, are shown in Figure 6B. The  $\text{Cd}^{2+}$ -sensitive currents showed time-dependent activation at hyperpolarization potentials (Figure 6A-d) and had an inwardly rectifying  $I$ - $V$  relationship with a mean reversal potential of  $-42.6 \pm 4.4$  mV ( $n=3$ ), which is very close to the estimated  $E_{\text{Cl}}$  ( $-45.6$  mV). These properties are very similar to those of  $I_{\text{Cl.ir}}$  observed in mouse cardiac myocytes under the same conditions (see Figure 2B). The TMX-sensitive currents (Figures 6A-e and 6D) were outwardly rectifying and had typical properties of  $I_{\text{Cl.vol}}$  in the same tissue described previously.<sup>10,31,42</sup> These results suggest that, in addition to the outwardly rectifying  $I_{\text{Cl.vol}}$ , hypotonic cell swelling also activates an inwardly rectifying  $I_{\text{Cl.ir}}$  in these guinea pig cardiac myocytes.

### Molecular Expression of ClC-2 in Mouse and Guinea Pig Heart

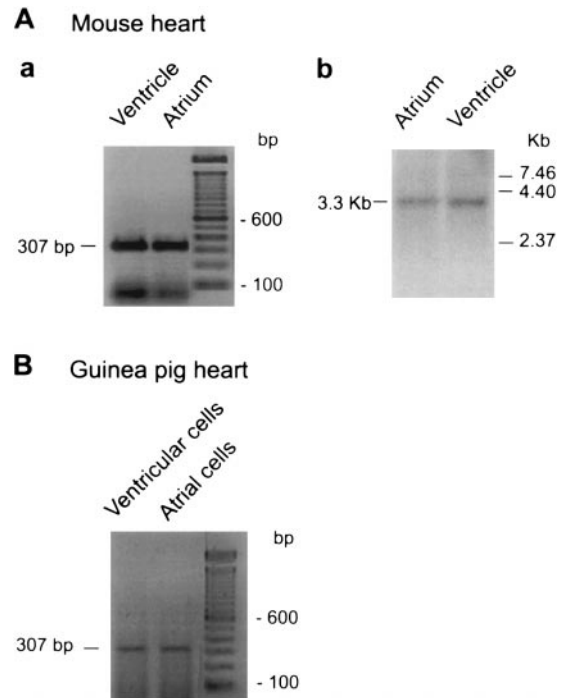
The biophysical and pharmacological properties of  $I_{\text{Cl.ir}}$  in mouse and guinea pig heart described above, including the anion selectivity, inward rectification, regulation by cell volume, sensitivity to 9-AC and  $\text{Cd}^{2+}$ , and insensitivity to SITS and TMX, are nearly identical to those known properties of currents generated by ClC-2 channels expressed in *Xenopus* oocytes<sup>19,20,45</sup> and mammalian HEK 293 cells,<sup>46</sup> suggesting that ClC-2 is a strong molecular candidate that may be responsible for  $I_{\text{Cl.ir}}$ . Therefore, we tested for molecular expression of ClC-2 in mouse and guinea pig heart.

Figure 7A shows an agarose gel depicting a ClC-2-specific RT-PCR product generated from RNA derived from mouse atrial and ventricular tissues. The RT-PCR reaction of total RNA prepared from both atrial and ventricular tissue with specific primers designed to amplify a 307-nucleotide of



**Figure 6.** Volume-regulated whole-cell anion currents in guinea pig atrial myocytes. Currents were recorded using the same low  $\text{Cl}^-$  (20 mmol/L) pipette as shown in Figure 2 and the same protocols as shown in Figure 3. A, Representative whole-cell currents recorded under hypotonic control (A-a), hypotonic  $0.3 \text{ mmol/L Cd}^{2+}$  (A-b), and hypotonic  $\text{Cd}^{2+}$  and  $10 \mu\text{mol/L TMX}$  (A-c) conditions. Panel A-d shows the  $\text{Cd}^{2+}$ -sensitive difference current obtained by subtracting the current in panel A-b from the current in panel A-a.  $\text{Cd}^{2+}$  inhibited a time-dependent inwardly rectifying current. Panel A-e shows the TMX-sensitive difference current obtained by subtracting the current in panel A-c from the current in panel A-b. TMX inhibited mainly the volume-regulated, outwardly rectifying  $\text{Cl}^-$  current ( $I_{\text{Cl,vol}}$ ; see text). B, Mean  $I$ - $V$  curves of whole-cell currents obtained from 3 different guinea pig ventricular myocytes under hypotonic (■), hypotonic  $\text{Cd}^{2+}$  (●), and hypotonic  $\text{Cd}^{2+}$ +TMX (▲) conditions. C, Mean  $I$ - $V$  curve of  $\text{Cd}^{2+}$ -sensitive whole-cell currents shows strong inward rectification and reversed at  $-42.6 \pm 4.4 \text{ mV}$  ( $n=3$ ), which is very close to the estimated  $E_{\text{Cl}}$  ( $-45.6 \text{ mV}$ ). D, Mean  $I$ - $V$  curve of TMX-sensitive currents exhibits strong outward rectification.

rCIC-2 (nucleotide positions 2515 to 2822, see Materials and Methods) confirmed the transcriptional expression of CIC-2 in both atrium and ventricle. The RT-PCR product was sequenced and determined to be identical to the previously cloned rCIC-2.<sup>20</sup> Northern blot analysis also indicated that CIC-2 mRNA is expressed in both atrial and ventricular tissue from mouse heart. Figure 7B shows hybridization to a transcript of  $\approx 3.3 \text{ kb}$ , which is similar in size to CIC-2 mRNA expressed in rat heart.<sup>20</sup> We also amplified a CIC-2-specific RT-PCR product generated from RNA derived from



**Figure 7.** Molecular expression of CIC-2 in mouse heart. A, Agarose gel depicting CIC-2-specific RT-PCR product from mouse atrial and ventricular tissue. The CIC-2-specific primers amplified a 307-nucleotide product of mouse CIC-2 (nucleotide positions 2515 to 2822), which confirmed transcriptional expression of CIC-2 in both atrial and ventricular cells. B, Northern analysis of CIC-2 expression in mouse cardiac tissues. Total RNA from atrial ( $20 \mu\text{g}$ ) and ventricular ( $20 \mu\text{g}$ ) tissue was hybridized with a  $^{32}\text{P}$ -labeled mouse CIC-2 probe (420 bp) as described in Materials and Methods. The mouse CIC-2 transcript was detected at  $\approx 3.3 \text{ kb}$ . C, Agarose gel depicting CIC-2-specific RT-PCR products generated from RNA derived from isolated ventricular and atrial myocytes enzymatically dispersed from guinea pig heart. Only rod-shaped myocytes with clear cross striations and no visible blebs on their surface were used for total RNA isolation. Sequence analysis of the products from RT-PCR of RNA isolated from these myocytes verified that transcripts identical to rCIC-2 were present in guinea pig atrial and ventricular myocytes.

isolated single atrial and ventricular myocytes enzymatically dispersed from guinea pig heart (Figure 7C). This RT-PCR reaction used the same specific primers and amplified a 307-nucleotide product of gpCIC-2, confirming transcriptional expression of CIC-2 in single atrial and ventricular myocytes.

## Discussion

In the present study, we first characterized the biophysical and pharmacological properties of a volume-regulated inwardly rectifying  $\text{Cl}^-$  current,  $I_{\text{Cl,ir}}$ , in mammalian heart. In both atrial and ventricular myocytes of mouse and guinea pig heart,  $I_{\text{Cl,ir}}$  activated slowly on hyperpolarization with a biexponential time course. The current was very sensitive to changes in cell volume. Whereas hypertonic cell shrinkage diminished the current, hypotonic cell swelling increased the current and accelerated the activation kinetics.  $I_{\text{Cl,ir}}$  exhibited strong inward rectification with a reversal potential close to the estimated  $E_{\text{Cl}}$  in symmetrical  $\text{Cl}^-$  and physiological

asymmetrical  $\text{Cl}^-$  conditions. The anion selectivity sequence of  $I_{\text{Cl.ir}}$  was  $\text{Cl}^- > \text{I}^- \gg \text{Asp}^-$ . Although  $I_{\text{Cl.ir}}$  was strongly blocked by  $\text{Cd}^{2+}$  and the carboxylic acid derivative, 9-AC, it was not sensitive to inhibition by effective blockers of  $I_{\text{Cl.vol}}$  such as TMX and the disulfonic stilbene derivative, SITS. All these properties clearly separate  $I_{\text{Cl.ir}}$  from other types of previously described  $\text{Cl}^-$  currents in heart, suggesting that  $I_{\text{Cl.ir}}$  may be mediated by a novel type of  $\text{Cl}^-$  channel.<sup>5</sup>

CIC-2 belongs to a large CIC gene family of voltage-gated  $\text{Cl}^-$  channels and is ubiquitously expressed in many tissues.<sup>9,20</sup> Initially, CIC-2 was cloned from rat heart and brain, but only the brain form was subsequently sequenced.<sup>20</sup> It has 907 amino acids, a molecular mass of  $\approx 99$  kDa, and shares  $\approx 50\%$  homology with CIC-0 and CIC-1. When transiently expressed in *Xenopus* oocytes, CIC-2 channels activate during hyperpolarization ( $-90$  to  $-180$  mV) and are further stimulated by cell swelling. CIC-2 channels exhibit a strong inwardly rectifying instantaneous  $I$ - $V$  relationship and an anion permeability of  $\text{Cl}^- \geq \text{Br}^- > \text{I}^-$ . The channel is blocked by carboxylic acid derivatives and  $\text{Cd}^{2+}$  but is largely unaffected by disulfonic stilbene derivatives and TMX.<sup>18-20,47</sup> When expressed in mammalian (HEK 293) cells, CIC-2 channels are active under isotonic conditions but exhibit faster activation kinetics than the channel expressed in *Xenopus* oocytes.<sup>46</sup> A rabbit homologue of CIC-2 (CIC-2G) was isolated from a rabbit gastric cDNA library.<sup>45</sup> CIC-2G has also been shown to be ubiquitously expressed in rabbit<sup>19,45</sup> and human<sup>48</sup> tissues. Recently, Furukawa et al<sup>49</sup> isolated a CIC-2 $\alpha$  clone from a rabbit heart cDNA library that is identical to CIC-2G. They also proposed that an alternatively spliced, truncated form of CIC-2, CIC-2 $\beta$ , may be specifically expressed in heart. However, in a subsequent study, they found this truncated CIC-2 $\beta$  clone is likely to be an artifact of library construction and not a product of alternative splicing.<sup>19</sup> It has been shown that, when expressed in *Xenopus* oocytes, CIC-2G (CIC-2 $\alpha$ ) channels have similar biophysical and pharmacological characteristics as rCIC-2 channels.<sup>19,45</sup>

$\text{Cl}^-$  currents with properties similar to those of heterologously expressed CIC-2 channels have not been specifically identified in native cardiac myocytes before, despite early reports of a hyperpolarization-activated  $\text{Cl}^-$  current in some multicellular cardiac preparations.<sup>26,28,50</sup> These results have generally been attributed to anion sensitivity of the hyperpolarization-activated  $I_f$  due to screening of positive charges near the external pore of the  $I_f$  channel<sup>51</sup> However, the hyperpolarization-activated inwardly rectifying currents observed in our experiments are unlikely due to  $I_f$  or other cationic inward rectifiers because (1) 10 mmol/L  $\text{Cs}^+$  and 2 mmol/L  $\text{Ba}^{2+}$  were included in the external bath solutions and the nonpermeable large cation NMDG was the only major cation in the internal pipette solutions, effectively precluding possible contamination from  $I_f$  and other cationic inward rectifiers, (2) the  $I$ - $V$  relationship was not altered by replacement of cations with NMDG and shifted as expected for a  $\text{Cl}^-$  selective channel when intracellular aspartate was substituted for  $\text{Cl}^-$ , and the measured reversal potentials of  $I_{\text{Cl.ir}}$  closely corresponded to the predicted value of  $E_{\text{Cl}}$ , (3) substitution of  $[\text{Cl}^-]_o$  by small anions such as  $\text{I}^-$  or  $\text{Asp}^-$

shifted the reversal potential of  $I_{\text{Cl.ir}}$  to positive potentials, consistent with a channel with a relative anion permeability of  $\text{Cl}^- > \text{I}^- \gg \text{Asp}^-$ , and (4)  $I_{\text{Cl.ir}}$  in cardiac myocytes was blocked by extracellular  $\text{Cd}^{2+}$ , an effective blocker of  $I_{\text{Cl.ir}}$  in many noncardiac cells. Recently, Clemons et al<sup>35</sup> have reported a nonspecific cationic inward rectifier current ( $I_{\text{Cir.swell}}$ ) that is also regulated by cell volume in rabbit ventricular myocytes and ventricular myocytes isolated from dog with tachycardia-induced congestive heart failure.<sup>36</sup> However,  $I_{\text{Cir.swell}}$  differs from  $I_{\text{Cl.ir}}$  in mouse and ventricular myocytes in that  $I_{\text{Cir.swell}}$  (1) does not show time-dependent activation at hyperpolarization potentials (see Figure 1 in Reference 35), (2) is not sensitive to changes in bath  $\text{Cl}^-$  concentrations, (3) is not sensitive to 9-AC, and (4) is dependent on extracellular cations and can be abolished by NMDG replacement for extracellular cations. Our results, therefore, clearly exclude the possibility that  $I_{\text{Cl.ir}}$  is the same as  $I_{\text{Cir.swell}}$ .

The properties of  $I_{\text{Cl.ir}}$  described in the present study are consistent with currents generated by CIC-2 channels, including the cardiac form CIC-2 $\alpha$ , when expressed in *Xenopus* oocytes<sup>19,20</sup> or mammalian cell lines.<sup>46</sup> Furthermore, we found that CIC-2 transcripts were present in both atrial and ventricular tissue and isolated single myocytes of mouse and guinea pig heart. Our results, therefore, provide the first compelling evidence for the functional expression of a novel  $\text{Cl}^-$ -dependent inward rectifier that may be encoded by the CIC-2 gene in native mammalian cardiac cells and support a potentially important role of CIC-2 in cardiac function.

**Possible Functional Role and Significance.** In general, the physiological role of CIC-2 channels remains uncertain because most studies have been carried out only on recombinant CIC-2 channels.<sup>9,18-20</sup> The volume sensitivity of the channel suggests some role in cell volume regulation. Volume regulatory mechanisms are critical in maintaining structural integrity and proper cellular functions of living cells. Cardiac myocytes, like other mammalian cells, are able to use a variety of mechanisms to precisely maintain their size in the face of osmotic perturbations. It is now well known that the outwardly rectifying  $I_{\text{Cl.vol}}$  plays a role in volume regulation of cardiac and noncardiac cells.<sup>52-56</sup> However, CIC-2 channels differ from the typical  $I_{\text{Cl.vol}}$  investigated in cardiac and noncardiac cells in terms of their anion selectivity, pharmacology, and rectification properties.<sup>5,9,10,18-20</sup> In fact,  $I_{\text{Cl.vol}}$  in heart, and possibly in other tissues as well, may be encoded by CIC-3.<sup>10</sup> Furukawa et al<sup>19</sup> recently found that CIC-2G (CIC-2 $\alpha$ ), when expressed in *Xenopus* oocytes, contributes to volume regulation in the face of osmotic perturbations. However, in human intestinal T84 cells, it was found that only the TMX-sensitive outwardly rectifying  $I_{\text{Cl.vol}}$  was involved in volume regulation but not the  $\text{Cd}^{2+}$ -sensitive inwardly rectifying CIC-2-like  $\text{Cl}^-$  current.<sup>33</sup> How CIC-2 channels are involved in the volume regulation of cardiac cells and their relationship to CIC-3 and other  $\text{Cl}^-$  channels involved in volume regulation, such as CFTR channels,<sup>57</sup> needs further investigation.

Considering the well-established physiological significance of cationic inward rectifiers like  $\text{Kir}^{58,59}$  and  $I_f^{21}$  in the regulation of resting membrane potential, action potential duration, and pacemaker activity, it is conceivable that



anionic inward rectifiers may also play a significant role in cardiac electrical activity. Under physiological conditions, the  $\text{Cl}^-$  equilibrium potential ( $E_{\text{Cl}}$ ) is more positive ( $-65$  to  $-30$  mV) than the resting membrane potential.<sup>60–62</sup> At negative membrane potentials, activation of CIC-2 channels would promote  $\text{Cl}^-$  efflux and the generation of significant inward current because of their inwardly rectifying properties, thus potentially contributing to the regulation of resting membrane potentials. In the present study, given that functional  $I_{\text{Cl,ir}}$  could only be demonstrated in a small percentage of isolated mouse and guinea pig atrial and ventricular myocytes, it may be that the physiological significance of these channels in these cell types only becomes prominent under some pathological conditions (ischemia or hypoxia).<sup>63</sup> It is possible that  $I_{\text{Cl,ir}}$  may normally play a much more prominent role in pacemaker cells in the sinoatrial or atrioventricular nodal regions of the heart, in a manner analogous to the physiological role of  $I_f$  channels and their known tissue distribution pattern in heart.<sup>22,64,65</sup> Future studies should be performed to examine functional and molecular expression of CIC-2 in nodal regions of the heart. Finally, additional functional significance of CIC-2 expression in some types of cardiac cells may be related to the formation of heteromultimers with other CIC  $\text{Cl}^-$  channel family subunits<sup>66</sup> to form unique, yet to be characterized,  $\text{Cl}^-$  channel subtypes.

### Acknowledgments

This study was supported by a grant-in-aid from the American Heart Association (D.D.). F.B. was supported by a fellowship from the Western States Affiliate of the American Heart Association, and B.H. and J.R.H. were supported by NIH grant HL52803.

### References

- Ackerman MJ, Clapham DE. Cardiac chloride channels. *Trends Cardiovasc Med.* 1993;3:23–28.
- Harvey RD. Cardiac chloride currents. *News Physiol Sci.* 1996;11:175–181.
- Hiraoka M, Kawano S, Hirano Y, Furukawa T. Role of cardiac chloride currents in changes in action potential characteristics and arrhythmias. *Cardiovasc Res.* 1998;40:23–33.
- Sorota S. Insights into the structure, distribution and function of the cardiac chloride channels. *Cardiovasc Res.* 1999;42:361–376.
- Hume JR, Duan D, Collier ML, Yamazaki J, Horowitz B. Anion transport in heart. *Physiol Rev.* 2000;80:31–81.
- Horowitz B, Tsung SS, Hart P, Levesque PC, Hume JR. Alternative splicing of CFTR  $\text{Cl}^-$  channels in heart. *Am J Physiol.* 1993;264:H2214–H2220.
- Gadsby DC, Nagel G, Hwang TC. The CFTR chloride channel of mammalian heart. *Annu Rev Physiol.* 1995;57:387–416.
- Hart P, Warth JD, Levesque PC, Collier ML, Geary Y, Horowitz B, Hume JR. Cystic fibrosis gene encodes a cAMP-dependent chloride channel in heart. *Proc Natl Acad Sci U S A.* 1996;93:6343–6348.
- Jentsch TJ, Friedrich T, Schriever A, Yamada H. The CLC chloride channel family. *Pflugers Arch.* 1999;437:783–795.
- Duan D, Winter C, Cowley S, Hume JR, Horowitz B. Molecular identification of a volume-regulated chloride channel. *Nature.* 1997;390:417–421.
- Duan D, Hume JR, Nattel S. Evidence that outwardly rectifying  $\text{Cl}^-$  channels underlie volume-regulated  $\text{Cl}^-$  currents in heart. *Circ Res.* 1997;80:103–113.
- Zhang K, Barrington PL, Martin RL, TenEick RE. Protein kinase-dependent  $\text{Cl}^-$  currents in feline ventricular myocytes. *Circ Res.* 1994;75:133–143.
- Collier ML, Hume JR. Unitary chloride channels activated by protein kinase C in guinea pig ventricular myocytes. *Circ Res.* 1995;76:317–324.
- Yamazaki J, Britton F, Collier ML, Horowitz B, Hume JR. Regulation of recombinant cardiac cystic fibrosis transmembrane conductance regulator chloride channels by protein kinase C. *Biophys J.* 1999;76:1972–1987.
- Middleton LM, Harvey RD. PKC regulation of cardiac CFTR  $\text{Cl}^-$  channel function in guinea pig ventricular myocytes. *Am J Physiol.* 1998;275:C293–C302.
- Duan D, Ye L, Britton F, Miller LJ, Yamazaki J, Horowitz B, Hume JR. Purinoceptor-coupled  $\text{Cl}^-$  channels in mouse heart: a novel, alternative pathway for CFTR regulation. *J Physiol (Lond).* 1999;521:43–56.
- Gandhi R, Eible RC, Gruber AD, Schreier KD, Ji HL, Fuller CM, Pauli BU. Molecular and functional characterization of a calcium-sensitive chloride channel from mouse lung. *J Biol Chem.* 1998;273:32096–32101.
- Grunder S, Thiemann A, Pusch M, Jentsch TJ. Regions involved in the opening of CIC-2 chloride channel by voltage and cell volume. *Nature.* 1992;360:759–762.
- Furukawa T, Ogura T, Katayama Y, Hiraoka M. Characteristics of rabbit CIC-2 current expressed in *Xenopus* oocytes and its contribution to volume regulation. *Am J Physiol.* 1998;274:C500–C512.
- Thieman A, Grunder S, Pusch M, Jentsch TJ. A chloride channel widely expressed in epithelial and non-epithelial cells. *Nature.* 1992;356:57–60.
- DiFrancesco D. Cardiac pacemaker: 15 years of “new” interpretation. *Acta Cardiol.* 1995;50:413–427.
- Shi W, Wymore R, Yu H, Wu J, Wymore RT, Pan Z, Robinson RB, Dixon JE, McKinnon D, Cohen IS. Distribution and prevalence of hyperpolarization-activated cation channel (HCN) mRNA expression in cardiac tissues. *Circ Res.* 1999;85:e1–e6.
- Santoro B, Liu DT, Yao H, Bartsch D, Kandel ER, Siegelbaum SA, Tibbs GR. Identification of a gene encoding a hyperpolarization-activated pacemaker channel of brain. *Cell.* 1998;93:717–729.
- Ludwig A, Zong X, Jeglitsch M, Hofmann F, Biel M. A family of hyperpolarization-activated mammalian cation channels. *Nature.* 1998;393:587–591.
- Gauss R, Seifert R, Kaupp UB. Molecular identification of a hyperpolarization-activated channel in sea urchin sperm. *Nature.* 1998;393:583–587.
- Seyama I. Characteristics of the anion channel in the sino-atrial node cell of the rabbit. *J Physiol (Lond).* 1979;294:447–460.
- Yanagihara K. Ionic current and pacemaker activity of the S-A node cells. *Jpn Circ J.* 1980;44:531–538.
- Yanagihara K, Irisawa H. Inward current activated during hyperpolarization in the rabbit sinoatrial node cell. *Pflugers Arch.* 1980;385:11–19.
- Duan D, Britton F, Ye L, Horowitz B, Hume JR. A novel anionic inward rectifier in cardiac myocytes encoded by CIC-2. *Biophys J.* 1999;76:A147. Abstract.
- Hamill OP, Marty A, Neher E, Sakmann B, Sigworth FJ. Improved patch-clamp techniques for high-resolution current recording from cells and cell-free membrane patches. *Pflugers Arch.* 1981;391:85–100.
- Duan D, Cowley S, Horowitz B, Hume JR. A serine residue in CIC-3 links phosphorylation-dephosphorylation to chloride channel regulation by cell volume. *J Gen Physiol.* 1999;113:57–70.
- Feinberg AP, Vogelstein B. A technique for radiolabeling DNA restriction endonuclease fragments to high specific activity. *Anal Biochem.* 1983;132:6–13.
- Bond TD, Ambikapathy S, Mohammad S, Valverde MA. Osmosensitive  $\text{Cl}^-$  currents and their relevance to regulatory volume decrease in human intestinal T84 cells: outwardly vs. inwardly rectifying currents. *J Physiol (Lond).* 1998;511(Pt 1):45–54.
- Enz R, Ross BJ, Cutting GR. Expression of the voltage-gated chloride channel CIC-2 in rod bipolar cells of the rat retina. *J Neurosci.* 1999;19:9841–9847.
- Clemo HF, Baumgarten CM. Swelling-activated  $\text{Gd}^{3+}$ -sensitive cation current and cell volume regulation in rabbit ventricular myocytes. *J Gen Physiol.* 1997;110:297–312.
- Clemo HF, Stambler BS, Baumgarten CM. Persistent activation of a swelling-activated cation current in ventricular myocytes from dogs with tachycardia-induced congestive heart failure. *Circ Res.* 1998;83:147–157.
- Hille B. The permeability of the sodium channel to organic cations in myelinated nerve. *J Gen Physiol.* 1971;58:599–619.
- Sorota S. Pharmacologic properties of the swelling-induced chloride current of dog atrial myocytes. *J Cardiovasc Electrophysiol.* 1994;5:1006–1016.
- Duan D, Nattel S. Properties of single outwardly rectifying  $\text{Cl}^-$  channels in heart. *Circ Res.* 1994;75:789–795.



40. Cabantchik ZI, Greger R. Chemical probes for anion transporters of mammalian cell membranes. *Am J Physiol.* 1992;262:C803–C827.
41. Vandenberg JI, Yoshida A, Kirk K, Powell T. Swelling-activated and isoprenaline-activated chloride currents in guinea pig cardiac myocytes have distinct electrophysiology and pharmacology. *J Gen Physiol.* 1994; 104:997–1017.
42. Shuba LM, Ogura T, McDonald TF. Kinetic evidence distinguishing volume-sensitive chloride current from other types in guinea-pig ventricular myocytes. *J Physiol (Lond).* 1996;491(Pt 1):69–80.
43. Vandenberg JI, Bett GC, Powell T. Contribution of a swelling-activated chloride current to changes in the cardiac action potential. *Am J Physiol.* 1997;273:C541–C547.
44. Sakaguchi M, Matsuura H, Ehara T. Swelling-induced  $\text{Cl}^-$  current in guinea-pig atrial myocytes: inhibition by glibenclamide. *J Physiol (Lond).* 1997;505(Pt 1):41–52.
45. Malinowska DH, Kupert EY, Bahinski A, Sherry AM, Cuppoletti J. Cloning, functional expression, and characterization of a PKA-activated gastric  $\text{Cl}^-$  channel. *Am J Physiol.* 1995;268:C191–C200.
46. Park K, Arreola J, Begenisich T, Melvin JE. Comparison of voltage-activated  $\text{Cl}^-$  channels in rat parotid acinar cells with CIC-2 in a mammalian expression system. *J Membr Biol.* 1998;163:87–95.
47. Jordt SE, Jentsch TJ. Molecular dissection of gating in the CIC-2 chloride channel. *EMBO J.* 1997;16:1582–1592.
48. Cid LP, Montrose-Rafizadeh C, Smith DI, Guggino WB, Cutting GR. Cloning of a putative human voltage-gated chloride channel (CIC-2) cDNA widely expressed in human tissues. *Hum Mol Genet.* 1995;4:407–413.
49. Furukawa T, Horikawa S, Terai T, Ogura T, Katayama Y, Hiraoka M. Molecular cloning and characterization of a novel truncated form (CIC-2 $\beta$ ) of CIC-2 $\alpha$  (CIC-2G) in rabbit heart [published erratum appears in *FEBS Lett.* 1997;403:1111]. *FEBS Lett.* 1995;375:56–62.
50. Noma A, Irisawa H. Membrane currents in the rabbit sinoatrial node cell as studied by the double microelectrode method. *Pflugers Arch.* 1976; 364:45–52.
51. Frace AM, Maruoka F, Noma A. Control of the hyperpolarization-activated cation current by external anions in rabbit sino-atrial node cells. *J Physiol (Lond).* 1992;453:307–318.
52. Hall SK, Zhang J, Lieberman M. Cyclic AMP prevents activation of a swelling-induced chloride-sensitive conductance in chick heart cells. *J Physiol (Lond).* 1995;488(Pt 2):359–369.
53. Garber S, Cahalan MD. Volume-regulated anion channels and the control of a simple cell behavior. *Cell Physiol Biochem.* 1997;7:229–241.
54. Nilius B, Eggermont J, Voets T, Buyse G, Manolopoulos V, Droogmans G. Properties of volume-regulated anion channels in mammalian cells. *Prog Biophys Mol Biol.* 1997;68:69–119.
55. Okada Y. Volume expansion-sensing outward-rectifier  $\text{Cl}^-$  channel: fresh start to the molecular identity and volume sensor. *Am J Physiol.* 1997; 273:C755–C789.
56. Strange K, Emma F, Jackson PS. Cellular and molecular physiology of volume-sensitive anion channels. *Am J Physiol.* 1996;270:C711–C730.
57. Wang Z, Mitsuiye T, Rees SA, Noma A. Regulatory volume decrease of cardiac myocytes induced by  $\beta$ -adrenergic activation of the  $\text{Cl}^-$  channel in guinea pig. *J Gen Physiol.* 1997;110:73–82.
58. Barry DM, Nerbonne JM. Myocardial potassium channels: electrophysiological and molecular diversity. *Annu Rev Physiol.* 1996;58:363–394.
59. Nichols CG, Lopatin AN. Inward rectifier potassium channels. *Annu Rev Physiol.* 1997;59:171–191.
60. Baumgarten CM, Fozzard HA. Intracellular chloride activity in mammalian ventricular muscle. *Am J Physiol.* 1981;241:C121–C129.
61. Desilets M, Baumgarten CM.  $\text{K}^+$ ,  $\text{Na}^+$ , and  $\text{Cl}^-$  activities in ventricular myocytes isolated from rabbit heart. *Am J Physiol.* 1986;251:C197–C208.
62. Vaughan-Jones RD. Chloride activity and its control in skeletal and cardiac muscle. *Philos Trans R Soc Lond B Biol Sci.* 1982;299:537–548.
63. Wright AR, Rees SA. Targeting ischaemia–cell swelling and drug efficacy [published erratum appears in *Trends Pharmacol Sci.* 1997; 18:345]. *Trends Pharmacol Sci.* 1997;18:224–228.
64. Robinson RB, Yu H, Chang F, Cohen IS. Developmental change in the voltage-dependence of the pacemaker current,  $I_t$ , in rat ventricle cells. *Pflugers Arch.* 1997;433:533–535.
65. Yu H, Chang F, Cohen IS. Pacemaker current  $I_t$  in adult canine cardiac ventricular myocytes. *J Physiol (Lond).* 1995;485(Pt 2):469–483.
66. Lorenz C, Pusch M, Jentsch TJ. Heteromultimeric CLC chloride channels with novel properties. *Proc Natl Acad Sci U S A.* 1996;93:13362–13366.

# Circulation Research

JOURNAL OF THE AMERICAN HEART ASSOCIATION



## A Novel Anionic Inward Rectifier in Native Cardiac Myocytes Dayue Duan, Lingyu Ye, Fiona Britton, Burton Horowitz and Joseph R. Hume

*Circ Res.* 2000;86:e63-e71

doi: 10.1161/01.RES.86.4.e63

*Circulation Research* is published by the American Heart Association, 7272 Greenville Avenue, Dallas, TX 75231

Copyright © 2000 American Heart Association, Inc. All rights reserved.

Print ISSN: 0009-7330. Online ISSN: 1524-4571

The online version of this article, along with updated information and services, is located on the  
World Wide Web at:

<http://circres.ahajournals.org/content/86/4/e63>

**Permissions:** Requests for permissions to reproduce figures, tables, or portions of articles originally published in *Circulation Research* can be obtained via RightsLink, a service of the Copyright Clearance Center, not the Editorial Office. Once the online version of the published article for which permission is being requested is located, click Request Permissions in the middle column of the Web page under Services. Further information about this process is available in the [Permissions and Rights Question and Answer](#) document.

**Reprints:** Information about reprints can be found online at:  
<http://www.lww.com/reprints>

**Subscriptions:** Information about subscribing to *Circulation Research* is online at:  
<http://circres.ahajournals.org/subscriptions/>